Food Chemistry 343 (2021) 128480

Contents lists available at ScienceDirect

Food Chemistry

journal homepage: www.elsevier.com/locate/foodchem

Investigating the migration of pyrethroid residues between mung bean sprouts and growth media

Wanwisa Wongmaneepratip [a], Hongshun Yang [a,b,*]

[a] Department of Food Science & Technology, National University of Singapore, Singapore 117542, Singapore
[b] National University of Singapore (Suzhou) Research Institute, 377 Lin Quan Street, Suzhou Industrial Park, Suzhou, Jiangsu 215123, PR China

ARTICLE INFO

Keywords:
Vegetable
Nanoparticle
Pesticide
Pesticide migration
Plant accumulation
Food safety
Food hazard
Rapid detection

ABSTRACT

To study the migration of pyrethroids (cypermethrin, deltamethrin, fenvalerate, and permethrin) from growth media (soil or water) to mung bean sprouts, pyrethroid residues were quantified using polystyrene-magnetic nanoparticles and HPLC-PDA. Pyrethroids reductions in growth media followed a double-exponential decline model (RMSE of 0.0068–0.1845), while the higher accumulation in the vegetable were observed in roots (0.50–6.75 mg/kg) than in sprouts (0.12–2.01 mg/kg). The accumulation was influenced by pyrethroid species, type of growth media, and plant parts. This study contributed a novel prediction method to assess the migration of pesticides from the growth media to the vegetable with the satisfactory sensitivity of the proposed detection method. The recoveries, detection limits (LOD), and quantification limits (LOQ) were 82.9–112.1%, 0.0627–0.1974 μg/L and 0.1892–0.6279 μg/L, respectively, for four pyrethroids. The research provided solid basis for future study of crops that can be used for bioconcentration of chemical hazards in environments.

1. Introduction

Pyrethroids are synthetic insecticides that are used widely in both agricultural and residential areas because of their high insecticidal activity and low toxicity toward mammals (Yoo, Lim, Kim, Lee, & Hong, 2016). However, many studies have demonstrated that exposure to pyrethroids can cause adverse effects and increase the risk to human health, for example, they may be mutagenic and carcinogenic to organisms and could affect the reproductive system, immune system, and nervous system (Han et al., 2017; Koureas, Tsakalof, Tsatsakis, & Hadjichristodoulou, 2012).

Although pyrethroids are mostly applied to crops, they can migrate and persist in soils because of their highly hydrophobic property (Bayen, Zhang, Desai, Ooi, & Kelly, 2013; Yu & Yang, 2017). Pesticides contaminated in soils can be taken up by plants depending on the type of plant, the structure of the pesticide, and the growing time, and the uptake amount relates to the pesticide concentration in their planted soils (Fantke, Wieland, Wannaz, Friedrich, & Jolliet, 2013; Hwang, Zimmerman, & Kim, 2018; Yang et al., 2019). In addition to soil contamination, pesticides used in both agricultural and urban areas can migrate to surface water via rain scouring, surface runoff, and drainage systems, resulting in water contamination (Mimbs, Cusaac, Smith, McMurry, & Belden, 2016; Nesser, Abdelbagi, Hammad, Tagelseed, & Laing, 2016). Many studies have considered the impact of pesticide-contaminated soils on crops. They have contributed plant uptake models to study the migration trends by growing plants in contaminated soils and have introduced a particular mathematical equation with complex parameters to predict the dynamics of plant pesticide uptake and transportation (Fantke et al., 2013; Hwang et al., 2018; Hwang, Lee, & Kim, 2017). However, to the best of authors' knowledge there is no study on the migration of pyrethroids from contaminated soil and contaminated water into plant. Pyrethroids contaminate in soils and water are a major concern for the safety of food and agricultural products because crops may take up pesticide residues from growth media and eventually enter our food chain. Therefore, there is a need to understand more about the migration and accumulation of pyrethroids among plant and its growth media. In this research, mung bean sprouts *(Vigna radiata)* are considered as an appropriate vegetable because they can cultivate individually in soil or water medium during a short period. Moreover, mung bean sprouts are extensively consumed as fresh and cooked vegetable in East Asia because of their high nutrition and convenience (Chen, Tan, Zhao, Yang, & Yang, 2019).

In terms of food safety, an extraction method is a crucial factor to effectively detect trace amounts of chemical contaminants in food or an

* Corresponding author at: Department of Food Science & Technology, National University of Singapore, Singapore 117542, Singapore.
E-mail address: fstynghs@nus.edu.sg (H. Yang).

https://doi.org/10.1016/j.foodchem.2020.128480
Received 19 October 2019; Received in revised form 17 October 2020; Accepted 22 October 2020
Available online 27 October 2020

environment. In the last decade, metal nanomaterials, such as magnetic nanoparticles, have been proposed as encouraging analytical adsorbents because of their low toxicity, ease of preparation, large surface area, and high selectivity (Alsammarraie, Wang, Zhou, Mustapha, & Lin, 2018; Bai et al., 2015; Xian et al., 2019). Yu and Yang (2017) have proved an effective property of magnetic nanoparticles coated with polystyrene on the extraction of pyrethroid residues in commercial vegetables. However, their application on pyrethroids quantification in environmental media such as soil and water are scarce. Thus, it is interested to extend an application of polystyrene-coated magnetic nanoparticles to detect trace amounts of pyrethroids in growth media.

There are several compounds of pyrethroids such as cypermethrin (CPM), deltamethrin (DMT), fenvalerate (FVL), and permethrin (PMT), have been detected more frequently and at high levels in environmental soils and water from various regions worldwide (Tang et al., 2018). Therefore, this research aimed to investigate the migration and accumulation of these pyrethroid residues in a vegetable-growth medium system by using polystyrene-coated magnetic nanoparticles based solid-phase extraction coupled with HPLC-PDA. Pyrethroids residues were determined in growth media collected from different stages and were also examined in mature sprouts at the end of the growth period. At last, this study provided a novel prediction method and evaluated values to assess the pyrethroids reduction in growth media and the pyrethroids accumulation in the vegetable.

2. Materials and methods

2.1. Chemicals and standards

Pyrethroid standards of cypermethrin (98.4%), deltamethrin (≥98.0%), fenvalerate (99.4%), and permethrin (98.3%) were acquired from Sigma Aldrich (St. Louis, MO, USA) and dissolved in acetonitrile. Commercial pesticides were obtained in form of an emulsifiable concentrate formulation of an active ingredient in inert ingredients. Commercial deltamethrin (2.8% w/w) and permethrin (18.7% w/w) were purchased from Bayer Thai Co., Ltd. (Bangkok, Thailand). Cypermethrin (15% v/v) and fenvalerate (10% w/v) were sourced from Wendell Trading Co. (Singapore) and Agricultural Chemicals (M) Sdn. Bhd. (Pinang, Malaysia), respectively.

Acetic acid, methanol, and high performance liquid chromatography (HPLC)-grade acetonitrile were obtained from Macron Fine Chemicals (Avantor, Radnor, PA, USA). A Milli-Q purification system was used to prepare deionised water. For nanoparticle synthesis, most of the chemicals, including concentrated hydrochloric acid (HCl), hydrated iron (II) chloride ($FeCl_2{\cdot}4H_2O$), methacrylic acid, oleic acid, potassium persulfate (KPS), sodium dodecylbenzenesulfonate (SDBS), and styrene were acquired from Sigma, while sodium hydroxide peal was obtained from Dickson Instrument & Reagent Store in Singapore and hydrated iron (III) chloride ($FeCl_3{\cdot}6H_2O$) was from Merck (Darmstadt, Germany).

2.2. Nanoparticle synthesis and characterisation

2.2.1. Magnetic nano-adsorbent particles (MNPs) preparation

The MNPs were synthesised based on method of Yu and Yang (2017). Briefly, 50 mL of deionised water, 4.4 g of $FeCl_2{\cdot}4H_2O$, 10.8 g of $FeCl_3{\cdot}6H_2O$, and 1.7 mL of hydrochloric acid (37% w/w) were mixed in dropwise funnel and then added into 500 mL of basic solution (NaOH, 1.5 M) at 70 °C under a vigorous stirrer system to prepare the core material, Fe_3O_4. After 2 h, the Fe_3O_4 material was separated and dispersed in 500 mL of deionised water. Then, 10 mL of oleic acid was added and stirred under the same conditions. After 0.5 h, 2.7 g of SDBS was added at room temperature and continuously stirred for 0.5 h to develop a colloidal solution. Then, 50 mL of the colloidal solution was mixed with 325 mL of deionised water, 22.5 mL of styrene, and 2.3 mL of methacrylic acid. Thereafter, a solution containing 375 mg of KPS and 6.25 mL of water was added to initiate the polystyrene coating at 70 °C using vigorous stirrer system for 6 h. All chemical reactions were performed under an N_2 atmosphere. The synthetic MNPs were washed with water (three times), with methanol (three times), and dried in an oven overnight.

2.2.2. MNPs characterisation and performance

To confirm the formation of the Fe_3O_4 core material, X-Ray diffraction (XRD) analysis using a Bruker-AXS D5005 instrument (Billerica, MA, USA) was applied. Moreover, Fourier Transform Infrared spectroscopy (FT-IR) was used to characterise the coating layer of the MNPs, which were prepared using the KBr pellet pressing method, before analysis on a Perkin Elmer Spectrum One FT-IR spectrometer (Waltham, MA, USA). The Vibrating Sample Magnetometer (VSM), Lakeshore model 7404 (Westerville, Ohio, USA) was performed to demonstrate the magnetic property of synthetic nanoparticles before and after coating with polystyrene. The magnetic curves were observed within a range of magnetic field (H) between −10,000 and 10,000 G, under the room temperature measurement. To evaluate the size and shape of core Fe_3O_4 nanoparticles and MNPs, the Transmission Electron Microscopy (TEM), a JEOL 3010 microscope, was employed. The sample was dispersed and diluted in ethanol with the assistance of ultrasonic for 20 min. The mix solution was dropped on a TEM grid (CF300-Cu-50, Carbon Film 300 Mesh) and left it dry under the room temperature before testing.

Furthermore, the recovery (%) rate, which is defined as the ratio of the analyte obtained from the spiked sample to the true concentration, were determined. In this study, each sample matrix (soil, water, and vegetable) were divided into two groups with six replicates of the non-spiked group (original sample) and the spiked group that were added with three levels of pyrethroids standard (0.1, 1.0, and 10.0 μg/g sample) before extraction. The analytes were extracted from these two group of samples by using the same extraction method. Then, the recovery rate was calculated as % Recovery rate = $[C_{sp} - C_{nsp}]*100/C_{std}$, where C_{sp} is the concentration of an analyte in spiked sample; C_{nsp} is the concentration of an analyte in non-spiked sample; and C_{std} is the concentration of standard added to the sample.

2.3. Growing methods and sample preparation

Organic mung bean seeds were grown in a plant-growth medium system with different treatments including contaminated soil (S treatments) and contaminated water (W treatments). Growth media were treated separately with individual commercial pyrethroids (CPM, DMT, FVL, or PMT) at low contamination level (LC) of 2 mg/kg soil or mg/L water, and high contamination level (HC) of 10 mg/kg soil or mg/L water. For the S treatment, 300 g of contaminated soil was placed in the bottom of pots, followed by 15 g of mung bean seed and another 200 g of soil, respectively. For the W treatment, the seeds were spread on a growing plate containing 500 mL of contaminated water. Soil and water samples from the S and W treatments were collected at 0, 12, 24, 36, 48, 60, and 72 h after planting. During the experimental period, no additional pyrethroids were applied. Mung bean sprouts were harvested at 72 h after planting in dark and divided into sprout and root parts. All samples were stored at −20 °C before analysis.

2.4. Pyrethroid residues extraction using MNPs

The extraction procedure was modified from Yu, Li, Ng, Yang, and Wang (2018). Briefly, 10 g of homogenised sprouts, roots, or soil sample was vortexed with 20 mL of acetonitrile for 5 min. The liquid-solid mixture was filtered and diluted with 80 mL of deionised water before vigorously stirring with 50 mg of MNPs for 20 min. Then, the MNPs attached with pyrethroids were separated using a permanent magnet and transferred to a 15 mL centrifuge tube. The pyrethroid residues on the MNPs were desorbed by adding 5 mL of the solution containing 3% acetic acid in acetonitrile with vortexing for 1 min. The eluent was purged with N_2 gas in a 40 °C water bath to dryness. The residue was

dissolved in 150 μL of acetonitrile and filtered through a 0.22-μm membrane filter before HPLC analysis. For the water samples, a similar approach was used without the filtration step. In comparison to other extraction and pre-concentration methods (Table S1), using the proposed method can provide good sensitivity with easily accessible instrument of HPLC-PDA. Moreover, the advantages with regard to the small amount of solvent and adsorbent use, the reusability of adsorbent, and applicable for various sample matrices were also presented.

2.5. HPLC analysis

Pyrethroids were analysed by a method modified from Yu and Yang (2017) using an HPLC instrument, Water 2695 Alliance system (Milford, MA, USA) supplied with a photodiode array (PDA) detector and a Luna 5μ C18 column of 150 mm × 4.6 mm, 10 nm pore size (Phenomenex, Torrance, CA, USA). A gradient system of 100% acetonitrile (A) and deionised water (B) was used to separate the four pyrethroid residues at a flow rate 1.00 mL/min and an injection volume of 10 μL. The mobile phase started with 68% A for 0–30 min, 75% A for 31–40 min, and 85% A for 45–50 min. For the PDA detector, the detection wavelength was set at 210 nm. An example of HPLC chromatograms of target pyrethroids extracted from water, sprout, and root samples presented in Fig. S1.

The quantification of pyrethroid residues in each sample was performed by using an external calibration curve method. The linearity of the calibration curves was studied by injecting triplicates of seven concentrations of mixed pyrethroid standards within the range of 1–10 μg/mL. The correlation coefficient of four target pyrethroids ranged from 0.9993 to 0.9999. The limit of detection (LOD) and quantification (LOQ) that refer to an accuracy of detected or quantified were also calculated using signal-to-noise ratios of S/N = 3 and S/N = 10, respectively. The range of LOD and LOQ were between 0.0627–0.1974 μg/L and 0.1892–0.6279 μg/L, respectively (Table S2).

2.6. Statistical analysis

All experiments were conducted in triplicate, excepting recoveries that were tested in six replicates. The mean and standard deviation (SD) were reported. Statistical analysis was performed using IBM SPSS version 22 computer software (IBM Corp., Armonk, NY, USA). A one-way analysis of variance (ANOVA; Duncan's multiple range test) with $P < 0.05$ was applied.

3. Results and discussion

3.1. Characterisation and performance of the MNPs

The XRD spectra (Fig. S2) of both the Fe_3O_4 core material and the MNPs showed characteristic peaks at 30.09°, 35.49°, 43.06°, 53.12°, 56.51°, and 62.48°, respectively, indicating the 220, 311, 400, 422, 511, and 440 crystal planes of an Fe_3O_4 crystal (Yu & Yang, 2017). Therefore, the Fe_3O_4 nanoparticles were completely synthesised via the co-precipitation method and retained their structure after coating with polystyrene.

According to the FT-IR spectrum (Fig. S3), the functional groups of the MNPs were identified to confirm that the polystyrene layer was successfully coated on the Fe_3O_4 nanoparticles. There was an absorption peak in both the raw Fe_3O_4 and MNPs samples at 579 cm^{-1}, which represented the stretching vibration of Fe-O within the Fe_3O_4 lattice. The existence of this peak also confirmed the successful synthesis of the core material Fe_3O_4. Furthermore, the FT-IR spectrum of the MNPs showed additional peaks at 700 cm^{-1}, which indicated the mono-substitution of benzene rings; the peaks at 1452, 1493, and 1600 cm^{-1} corresponded to the bending vibration of —C═C— on benzene rings; the absorption peaks at 2852 and 2923 cm^{-1} indicated the C—H symmetrical and asymmetrical stretching vibration, respectively; while the peaks found at 3025 and 3059 cm^{-1} corresponded to the ═CH stretching vibration on benzene rings (Yu et al., 2018). The presence of these addition peaks demonstrated that the Fe_3O_4 nanoparticles were successfully coated with polystyrene.

The magnetic curves of Fe_3O_4 nanoparticles and MNPs, showed in Fig. S4, demonstrated a strong magnetisation without hysteresis loop. This confirmed that after coating with polystyrene, MNPs still preserve their magnetic property and could be easily separated by a magnet once dispersed in the extracted solution (Wang et al., 2014). Within the range of magnetic field (H) −10,000 to 10,000 G, the magnetic saturation of Fe_3O_4 and MNPs were 0.51 emu and 0.27 emu, respectively. A decreasing of the magnetic saturation in MNPs was obviously caused by the coating of polystyrene on nanoparticle surface, which is another evidence to prove the successful synthesis of MNPs.

According to the TEM images presented in Fig. S5, Fe_3O_4 nanoparticles and MNPs showed sphere like shape with an average diameter of 20 nm. The small size of particles provided an advantage of high surface area to volume ratio that is an essential property for analytes adsorption during extraction process (Xian et al., 2019). The magnetic properties of nanoparticles caused an aggregation of particles demonstrated in TEM images.

To measure the MNPs performance, pyrethroid concentrations in soil, water, and mung bean sprouts spiked with mixed pyrethroid standards at 0.1, 1.0 and 10.0 μg/g sample, were determined and the recovery values ranged from 82.9 to 112.1%, with the standard deviation of 6.2–12.6% (Table 1).

3.2. Pyrethroid residues in growth media

The initial concentration (0 h) of an individual pyrethroid (CPM, FVL, PMT, and DMT) in S treatments (contaminated soil) ranged from 1.91 to 2.45 mg/kg soil and 9.21–10.62 mg/kg soil for LC and HC levels, respectively. Besides, their concentrations in W treatments (contaminated water) were 1.92–2.25 mg/L water and 9.98–10.42 mg/L water for the LC and HC levels, respectively. Throughout the growth period, pyrethroids reductions in growth media were determined and are presented in Table 2 with the statistical analysis in Table S3. In addition, the percentage reduction, compared between a pyrethroid concentration in the growth medium at 0 h and 72 h, are also indicated. A greater reduction in pyrethroid levels was observed for the LC-W treatments (CPM 71.96%; FVL 70.15%; PMT 32.99%; and DMT 52.20%) and HC-W treatments (CPM 38.94%; FVL 49.56%; PMT 17.44%; and DMT 61.76%) compared with those for the LC-S treatments (CPM 63.73%; FVL 19.81%; PMT 23.58%; and DMT 25.89%) and HC-S treatments (CPM

Table 1
The recovery (%) using synthetic nanoparticles to extract pyrethroid residues from soil, water, and plant matrices.

Target compound	Spiked concentration (μg/g)	Soil sample (n = 6)	Water sample (n = 6)	Plant sample (n = 6)
		(%) Recovery ± SD	(%) Recovery ± SD	(%) Recovery ± SD
Cypermethrin (CPM)	0.1	88.2 ± 8.9	103.3 ± 9.8	91.7 ± 9.7
	1	98.5 ± 11.9	107.8 ± 11.8	102.0 ± 11.2
	10	103.6 ± 10.2	112.3 ± 10.3	109.4 ± 9.2
Fenvalerate (FVL)	0.1	82.9 ± 9.6	89.2 ± 8.7	96.1 ± 9.7
	1	86.8 ± 6.2	96.3 ± 8.6	97.2 ± 9.3
	10	95.1 ± 9.7	103.4 ± 8.7	100.9 ± 8.3
Permethrin (PMT)	0.1	97.2 ± 8.1	104.5 ± 9.5	99.4 ± 7.1
	1	101.7 ± 6.2	107.2 ± 5.7	103.6 ± 6.5
	10	111.6 ± 8.3	112.1 ± 8.7	110.5 ± 9.7
Deltamethrin (DMT)	0.1	84.9 ± 10.0	89.2 ± 9.5	92.6 ± 9.9
	1	94.1 ± 8.8	98.4 ± 12.6	96.3 ± 10.1
	10	102.2 ± 7.7	108.3 ± 11.5	110.2 ± 10.7

Table 2
Pyrethroid concentrations in growth media.

Treatment	Collecting time	Pyrethroid concentration (mg/kg soil or mg/L water)			
		CPM	FVL	PMT	DMT
LC-S	0 (h)	2.04 ± 0.13^{d}	2.12 ± 0.03^{c}	2.12 ± 0.18^{d}	2.24 ± 0.21^{b}
	12	1.21 ± 0.07^{c}	2.07 ± 0.04^{c}	2.06 ± 0.06^{d}	2.18 ± 0.09^{b}
	24	0.99 ± 0.05^{b}	2.05 ± 0.25^{c}	2.00 ± 0.16 ^{cd}	2.15 ± 0.18^{b}
	36	0.91 ± 0.05^{ab}	1.97 ± 0.03^{bc}	1.91 ± 0.12^{bcd}	2.08 ± 0.08^{b}
	48	0.83 ± 0.15^{ab}	1.89 ± 0.17^{abc}	1.82 ± 0.13^{abc}	2.02 ± 0.23^{b}
	60	0.80 ± 0.02^{ab}	1.80 ± 0.05^{ab}	1.70 ± 0.04^{ab}	1.74 ± 0.07^{a}
	72	0.74 ± 0.17^{a}	1.70 ± 0.06^{a}	1.62 ± 0.04^{a}	1.66 ± 0.15^{a}
	%Reduction	63.73%	19.81%	23.58%	25.89%
LC-W	0 (h)	2.14 ± 0.11^{d}	2.01 ± 0.04^{f}	1.97 ± 0.05^{e}	2.05 ± 0.04^{e}
	12	1.12 ± 0.10^{c}	1.75 ± 0.05^{e}	1.62 ± 0.07^{d}	1.58 ± 0.06^{d}
	24	0.87 ± 0.05^{b}	1.51 ± 0.03^{d}	1.46 ± 0.04^{c}	1.37 ± 0.07^{c}
	36	0.84 ± 0.03^{b}	1.03 ± 0.03^{c}	1.42 ± 0.05^{bc}	1.35 ± 0.03^{c}
	48	0.81 ± 0.05^{b}	0.84 ± 0.09^{b}	1.40 ± 0.05^{abc}	1.23 ± 0.03^{b}
	60	0.69 ± 0.03^{a}	0.68 ± 0.04^{a}	1.36 ± 0.01^{ab}	1.07 ± 0.07^{a}
	72	0.60 ± 0.06^{a}	0.60 ± 0.02^{a}	1.32 ± 0.02^{a}	0.98 ± 0.06^{a}
	%Reduction	71.96%	70.15%	32.99%	52.20%
HC-S	0 (h)	9.46 ± 0.25^{f}	10.12 ± 0.31^{c}	10.30 ± 0.32^{c}	10.14 ± 0.08^{c}
	12	9.08 ± 0.10^{e}	10.06 ± 0.22^{c}	10.02 ± 0.29^{bc}	10.11 ± 0.04^{c}
	24	8.75 ± 0.21^{d}	9.88 ± 0.05^{bc}	10.00 ± 0.18^{bc}	10.06 ± 0.30^{bc}
	36	8.39 ± 0.13^{c}	9.71 ± 0.10^{b}	9.71 ± 0.10^{b}	9.74 ± 0.05^{b}
	48	7.62 ± 0.18^{b}	9.55 ± 0.22^{b}	9.23 ± 0.17^{a}	9.38 ± 0.31^{a}
	60	6.97 ± 0.13^{a}	9.03 ± 0.03^{a}	8.97 ± 0.04^{a}	9.16 ± 0.06^{a}
	72	6.88 ± 0.14^{a}	8.78 ± 0.18^{a}	8.90 ± 0.16^{a}	9.09 ± 0.24^{a}
	%Reduction	27.27%	13.24%	13.59%	10.36%
HC-W	0 (h)	10.04 ± 0.05^{g}	10.19 ± 0.08^{g}	10.15 ± 0.15^{f}	10.20 ± 0.22^{g}
	12	8.00 ± 0.04^{f}	8.56 ± 0.08^{f}	9.80 ± 0.06^{e}	8.31 ± 0.05^{f}
	24	7.31 ± 0.11^{e}	7.51 ± 0.04^{e}	9.31 ± 0.09^{d}	7.08 ± 0.03^{e}
	36	7.16 ± 0.04^{d}	6.83 ± 0.04^{d}	8.92 ± 0.08^{c}	6.05 ± 0.05^{d}
	48	6.75 ± 0.05^{c}	5.87 ± 0.08^{c}	8.58 ± 0.05^{b}	4.58 ± 0.09^{c}
	60	6.52 ± 0.04^{b}	5.62 ± 0.04^{b}	8.43 ± 0.02^{a}	4.25 ± 0.05^{b}
	72	6.13 ± 0.09^{a}	5.14 ± 0.03^{a}	8.38 ± 0.02^{a}	3.90 ± 0.04^{a}
	%Reduction	38.94%	49.56%	17.44%	61.76%

LC = low concentration treatment (2 mg/kg soil or mg/L water); HC = high concentration treatment (10 mg/kg soil or mg/L water).
Three replication for each treatment. S = Contaminated soil treatment; W = Contaminated water treatment.
CPM = cypermethrin; FVL = fenvalerate; PMT = permethrin; DMT = deltamethrin.
^{a,b,c,d,e,f,g} Different lower case letters in a column indicate significant differences between mean values of the concentrations evaluated by Duncan's multiple range test ($P < 0.05$).

27.27%; FVL 13.24%; PMT 13.59%; and DMT 10.36%), respectively.

During seven-time points (0–72 h) of collecting samples, the reductions of pyrethroid residues in S treatments showed only a few points of significant differences, compared to W treatments (Table 2). This is because of the possible attractions between pesticides and soil particles or soil organic matter (Fig. 1). Pesticides have an affinity for, and bind to, soil via different types of interactions such as sorption, electrostatic interactions, covalent bonding, or combinations of these interactions (Bollag, Myers, & Minard, 1992; Hanson, Hallman, Bond, & Jenkins, 2017). The strength of attraction can be influenced by many factors, for instance, pH, chemical compositions of the soil, and physical and chemical properties of the pesticides (Hanson, Hallman, Bond, & Jenkins, 2017; Senesi & Loffredo, 2008). Ahmed, Kühn, Aziz, Hilal, and Leinweber (2014) mentioned that hydrophobic pollutants can be adsorbed and remain in soil components, especially organic matter, rather than in aqueous systems. However, the interactions at the molecular level between pesticides and soil or water are not well understood.

The reduction curves of individual pyrethroids in growth media were plotted according to three equation models, including a double-exponential decline model (Eq. (1)), first-order (Eq. (2)), and second-order (Eq. (3)) kinetic models. The model equations proposed by Hwang et al. (2018) and Zimmerman, Gao, and Ahn (2011) are expressed as:

$$C_s(t) = C_0 - \left[P_1\left(1 - e^{-k_1 t}\right) + P_2\left(1 - e^{-k_2 t}\right)\right] \quad (1)$$

$$C_s(t) = C_0 \times e^{-k_f t} \quad (2)$$

$$C_s(t) = C_0/(1 + C_0 k_s t) \quad (3)$$

where $C_s(t)$ is the pyrethroid concentration in the growth medium at different time points (mg/kg medium); C_0 is the initial pyrethroid concentration in the growth medium at time zero (mg/kg medium); P_1 and P_2 are ratios of the labile and stable phase of pyrethroid decline (%), respectively; k_1 and k_2 are the apparent first-order depletion rate constants at the first and second depletion phases (h^{-1}), respectively; k_f and k_s are the apparent first- and second-order rate constants (h^{-1}), respectively; and t is the time point during the growth period (h).

For the sake of simplicity, only the means of triplicate values of pyrethroid concentrations in growth media were plotted at each time point. Moreover, the model parameter values were estimated using the Solver add-in tool in Microsoft Excel™ to minimise the differences between the modeled and measured values. The results showed that the values of root mean square error (RMSE) obtained from the regressions of a double-exponential decay model (RMSE of 0.0068 to 0.1721) were lower than those of a first-order model (RMSE of 0.0251 to 0.4731) and a second-order model (RMSE of 0.0338 to 0.4306). In addition, the correlation coefficients (R^2) of the double-exponential decay, first-order, and second-order models ranged from 0.8728 to 0.9997, 0.7913 to 0.9821, and 0.8310 to 0.9925, respectively (Table 3). These values confirmed that a double-exponential decay model is an appropriate equation to describe the reduction trends of all pyrethroids in both LC-W and HC-W treatments. Hwang et al. (2018) and Fantke et al. (2013) also proposed that the decreasing trend of pesticides such as endosulfan (ED), cyromazine, and carbaryl in growth medium over the experimental period could be explained by exponential equations. A double-exponential decay model might also be used to describe the pyrethroid decline trends in the LC-S and HC-S treatments; however, these trends were not obvious because some of LC-S and HC-S treatments presented only two or three significantly different points of pyrethroid concentrations during the growth period (Table 2). The binding affinity between the pesticide and soil organic matter might play an important role in the insignificant reductions of pyrethroids in soil medium.

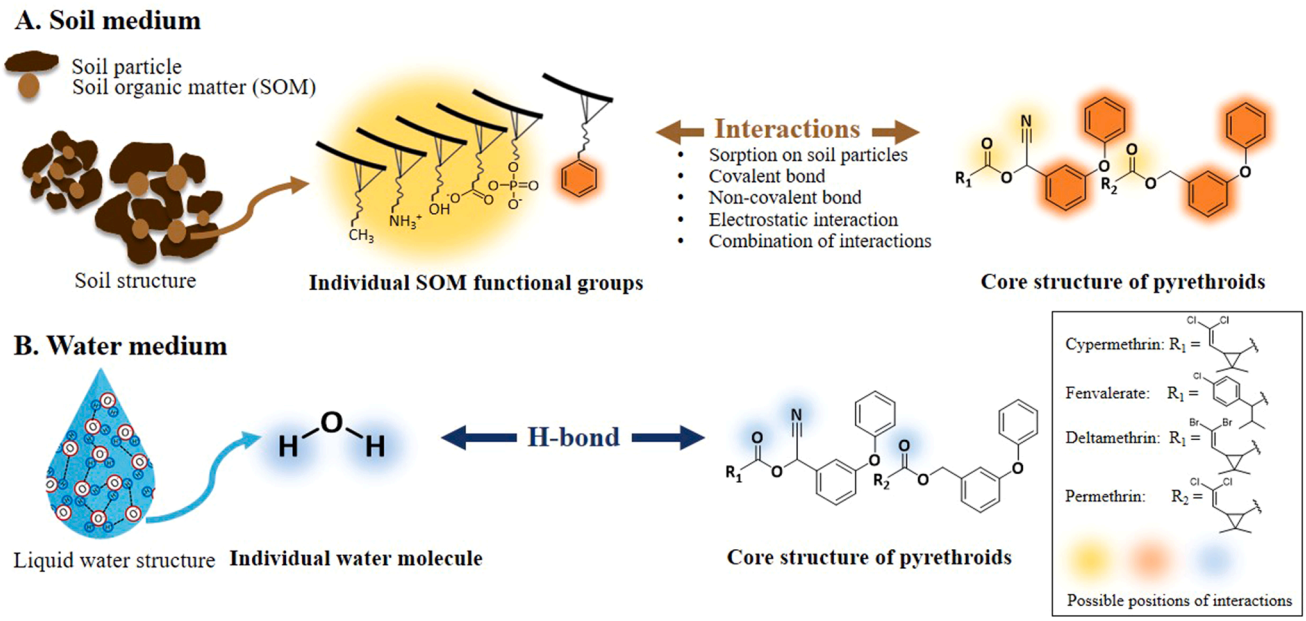

Fig. 1. Schematic interactions between the potential functional groups of pyrethroids and soil organic matter (SOM) or water molecules. (A) In soil, pyrethroids may attach to the surface of soil particles and bind to soil organic matter via many types of interaction, such as sorption, covalent bonding, and electrostatic interaction. (B) In water, pyrethroids may bind to water molecules via hydrogen bonding (SOM adapted from Newcomb, Qafoku, Grate, Bailey, & De Yoreo, 2017).

Table 3
The root mean square error (RMSE) and correlation coefficient (R^2) of reduction curves according to the different kinetic models.

Kinetic model	Treatment	Root mean square error (RMSE)				Correlation coefficient (R^2)			
		CPM	FVL	PMT	DMT	CPM	FVL	PMT	DMT
First-order									
	LC-S	0.2080	0.0303	0.0251	0.0749	0.8034	0.9568	0.9802	0.8767
	LC-W	0.2509	0.0776	0.0979	0.0921	0.8064	0.9821	0.7913	0.9430
	HC-S	0.1722	0.1306	0.1076	0.1110	0.9666	0.9256	0.9570	0.9355
	HC-W	0.4731	0.2613	0.1308	0.2472	0.8673	0.9769	0.9551	0.9790
Second-order									
	LC-S	0.1947	0.0353	0.0338	0.0853	0.9024	0.9453	0.9700	0.8578
	LC-W	0.2279	0.2572	0.0931	0.0720	0.9153	0.9700	0.8310	0.9686
	HC-S	0.2071	0.1434	0.1542	0.1313	0.9568	0.9170	0.9547	0.9344
	HC-W	0.4306	0.1413	0.1250	0.3179	0.9127	0.9925	0.9612	0.9809
Double exponential									
	LC-S	0.0068	0.0303	0.0252	0.0741	0.9997	0.9551	0.9791	0.8728
	LC-W	0.0304	0.0766	0.0112	0.0327	0.9961	0.9777	0.9973	0.9903
	HC-S	0.1721	0.1310	0.1077	0.1115	0.9672	0.9243	0.9565	0.9322
	HC-W	0.0626	0.0955	0.0709	0.1845	0.9974	0.9968	0.9879	0.9927

LC = low concentration level (2 mg/kg soil or mg/L water); HC = high concentration level (10 mg/kg soil or mg/L water).
S = Contaminated soil treatment; W = Contaminated water treatment.
CPM = cypermethrin; FVL = fenvalerate; PMT = permethrin; DMT = deltamethrin.

3.3. Pyrethroid concentrations in sprout and root samples

Mung bean sprouts were harvested from LC-S, LC-W, HC-S, and HC-W treatments after 72 h of the growth period and then separated into sprout and root parts. Pyrethroid concentrations in the individual plant parts were determined and are shown in Table 4. The results demonstrated that pyrethroid residues in contaminated soil (S treatments) and contaminated water (W treatments) were taken up by mung bean sprouts, and their concentrations in the sprout and root parts increased with the increasing pyrethroid concentrations in the growth media (LC and HC levels). In other plants such as persimmon and jujube, the pyrethroid levels in crops also increased as pyrethroid concentrations increased in their growing soils; however, the correlation was not linear (Liu et al., 2016). The plant uptake of pesticides from growth media can occur via different pathways, for instance through water absorption systems, diffusion across the plant's surface cuticle, and penetration into plant tissues (Hwang, Lee, & Kim, 2015; Juraske et al., 2011; Trapp, Cammarano, Capri, Reichenberg, & Mayer, 2007; Yang et al., 2016).

Concentrations of CPM, FVL, PMT, and DMT in sprouts were 0.20–1.60 mg/kg sprout, 0.10–1.20 mg/kg sprout, 0.03–0.50 mg/kg sprout, and 0.22–2.01 mg/kg sprout, respectively. Compared with the results for the sprouting part grown under the same treatment, the concentrations of CPM, FVL, PMT, and DMT in root were higher, at 0.50–5.37 mg/kg root, 0.50–4.29 mg/kg root, 0.21–4.11 mg/kg root, and 0.77–6.75 mg/kg root, respectively. Other researchers have reported the high levels of pesticides and other hydrophobic pollutants in the root parts of plants. Eggen, Heimstad, Stuanes, and Norli (2013) indicated that high levels of organophosphates and other hydrophobic

Table 4
Pyrethroid concentrations in sprout and root samples from different treatments.

Plant part	Treatment	Pyrethroid concentration (mg/ kg plant)			
		CPM	FVL	PMT	DMT
Sprout	LC-S	0.20 ± 0.04[b]	0.19 ± 0.02[b]	0.12 ± 0.03[a]	0.23 ± 0.03[b]
	LC-W	0.23 ± 0.04[c]	0.10 ± 0.02[b]	0.03 ± 0.01[a]	0.22 ± 0.03[c]
	HC-S	0.25 ± 0.03[a]	0.59 ± 0.15[b]	0.31 ± 0.07[a]	0.72 ± 0.02[b]
	HC-W	1.60 ± 0.02[c]	1.20 ± 0.03[b]	0.50 ± 0.03[a]	2.01 ± 0.06[d]
Root	LC-S	0.50 ± 0.10[b]	0.50 ± 0.03[b]	0.21 ± 0.05[a]	0.77 ± 0.04[c]
	LC-W	0.89 ± 0.06[c]	0.80 ± 0.03[b]	0.46 ± 0.05[a]	1.22 ± 0.03[d]
	HC-S	0.76 ± 0.20[a]	3.26 ± 0.33[c]	1.64 ± 0.10[b]	4.73 ± 0.52[d]
	HC-W	5.37 ± 0.08[b]	4.29 ± 0.09[a]	4.11 ± 0.05[a]	6.75 ± 0.16[c]

LC = low concentration level (2 mg/kg soil or mg/L water); HC = high concentration level (10 mg/kg soil or mg/L water).
S = Contaminated soil treatment; W = Contaminated water treatment.
Three replication for each treatment.
CPM = cypermethrin; FVL = fenvalerate; PMT = permethrin; DMT = deltamethrin.
[a,b,c,d] Different lower case letters in a row indicate significant differences between mean values of the concentrations evaluated by Duncan's multiple range test ($P < 0.05$).

substances persisted in the roots of food and forage crops. In addition, the highest concentration of pesticides, imidacloprid (Juraske, Castells, Vijay, Muñoz, & Antón, 2009) and endosulfan (Hwang et al., 2018), were found in roots rather than in other plant parts, such as the stem and fruit. Significant amounts of pesticides are absorbed from growth media and are mostly retained in the roots, while some of residues are transferred to other plant parts (Hwang et al., 2015; Paustenbach & Madl, 2008). During plant development, the roots are commonly the first part that contacts with pesticides in the growth medium and pesticide uptake through the roots is a normal process of absorption; therefore, plant roots are the major contaminated parts.

Under the same contamination level (LC or HC), mung bean sprouts growing in W treatments contained higher levels of pyrethroids (total concentration in sprout and root) than samples collected from S treatments. This result illustrated that the uptake of pyrethroids by mung bean sprouts from water medium was greater than that taken up from soil medium. Plants absorb large amounts of water for their development or germination; therefore, pyrethroids dispersed in water tend to be taken up by plants more easily than those that persist in soil (Fig. 1). In addition, the interaction or binding between water and pyrethroids might not be strong because of the hydrophobicity of pyrethroids, which would accumulate or bind to hydrophobic substances in mung bean sprouts (Pereira, Rodrigues da Cunha, Morais, Oliveira, & Morais, 2016).

In sprout and root parts growing under the same treatments, PMT tended to be detected at the lowest levels compared with CPM, FVL, and DMT, excepting the root part growing in HC-S treatment where CPM was monitored as the lowest level followed by PMT. This result revealed a relationship between the pyrethroid concentrations in plants and that in the growth media. A small amount of PMT was absorbed by plants; therefore, a high level of PMT still remained in the growth media (Table 2). For instance, the PMT concentrations in sprouts and roots of mung beans grown in the HC-W treatment were 0.50 ± 0.03 mg/kg sprout and 4.11 ± 0.05 mg/kg root, respectively, and the percent reduction of PMT in the water medium was 17.44%. Meanwhile, the DMT levels in sprouts and roots were 2.10 ± 0.06 mg/kg sprout and 6.75 ± 0.16 mg/kg root, respectively, and the percent reduction of DMT in the water medium reached 61.76%. Based on the results of the present study, plant uptake plays an important role in the changing of pyrethroid levels in growth media. The chemical and physical properties of pesticides are the major factors that influence plant uptake levels. Plants can easily absorb pesticides and organic pollutants with a molecular mass below 1 kg/mol and with a high value of the octanol:water partition coefficient (K_{ow}) (Kvesitadze, Khatisashvili, Sadunishvili, & Kvesitadze, 2015; Liu & Schnoor, 2008). The K_{ow} is a crucial value related to the solubility of a substance in two immiscible phases, *n*-octanol and water. Pesticides with a high K_{ow}, such as hydrophobic compounds, are highly accumulated in plants because of their affinity to the lipophilic components of plants (Pereira et al., 2016). According to the K_{ow} values, PMT (1.3×10^6) had a lower K_{ow} than FVL (1.6×10^6), DMT (3.4×10^6), and CPM (3.5×10^6) (Adelsbach & Tjeerdema, 2003; Laskowski, 2002; Zhang et al., 2017); therefore, mung bean sprouts might find it more difficult to absorb PMT compared with the other pyrethroids used in this study.

3.4. Bioconcentration factor (BCF) and $C_{s,\ permission}$

The bioconcentration factor (BCF) is described as the ability of plants to accumulate the substrate from the surrounding environment (Mishra & Pandey, 2019). Using the experimental data from Tables 2 and 4, the BCFs were calculated as the ratio of the pyrethroid concentration in the particular plant part at the harvest date to that in the growth medium at the planting date (Eq. (4)) and the results are presented in Table 5.

$$BCF_t = C_p(t)/C_s \quad (4)$$

where $C_p(t)$ is a pyrethroid concentration in the particular plant part (sprout or root) at the harvest time (mg/kg plant part); and C_s is a pyrethroid concentration in the growth medium at the planting time.

The BCF values of each pyrethroid in plant roots were greater than those in the sprout parts, growing under the same treatment, probably because of the higher ability of roots to absorb pesticides (higher pyrethroid concentrations were detected in plant roots). The comparable BCFs of individual pyrethroids between the LC and HC levels under the same growing medium showed that the accumulations of pyrethroids in sprouts and roots tended to increase with the increased initial pyrethroid concentration in the growth media. Similar results were reported by Hwang et al. (2018), in which the pesticide concentrations in potatoes correlated positively with the initial concentrations of the pesticide in soil.

In addition, the permissible concentrations of pyrethroids in growth media ($C_{s,\ permissible}$) were calculated as follows (Hwang et al., 2018):

$$C_{s,permissible} = MRL/BCF_t \quad (5)$$

where MRL is the maximum pesticide residue limits in crops based on the SFA regulations (Agency, 2020), and the BCF_t was calculated by using Eq. (4).

The $C_{s,\ permissible}$ (mg/kg soil or mg/L) values shown in Table 5 were the estimated maximum concentrations of pyrethroids in the growth media at the time of planting that would produce mung bean sprouts with pyrethroid concentrations lower than their MRLs (0.05 mg/kg plant for individual pyrethroids). For soil medium, the $C_{s,\ permissible}$ of CPM, FVL, PMT, and DMT were 0.21–1.91 mg/kg soil, 0.16–0.89 mg/kg soil, 0.31–1.71 mg/kg soil, and 0.11–0.71 mg/kg soil, respectively. For water medium, the $C_{s,\ permissible}$ of CPM (0.09–0.47 mg/L), FVL (0.12–1.03 mg/L), PMT (0.12–3.54 mg/L), and DMT (0.08–0.47 mg/L) tended to be lower than those in soil medium because mung bean sprouts could more effectively absorb pyrethroids from the water medium than the soil medium. These results suggested that it should be possible to produce mung bean sprouts with safe levels of pyrethroids, when the initial concentrations of CPM, FVL, PMT, and DMT in soil and water are below 0.21, 0.16, 0.31, and 0.11 mg/kg soil and below 0.09, 0.12, 0.12, and 0.08 mg/L water, respectively. Regarding the

Table 5
Calculated bioconcentration factor (BCF_t) at the harvest time and the permissible concentrations ($C_{s,\ permissible}$) of pyrethroids in sprout and root samples.

Plant part	Treatment	*BCF_t at harvest day				**C_s, permissible; mg/kg or mg/L			
		CPM	FVL	PMT	DMT	CPM	FVL	PMT	DMT
Sprout	LC-S	0.098 ± 0.013^{b}	0.090 ± 0.008^{b}	0.056 ± 0.009^{a}	0.102 ± 0.004^{b}	0.520 ± 0.073^{a}	0.562 ± 0.052^{a}	0.909 ± 0.157^{b}	0.489 ± 0.019^{a}
	LC-W	0.107 ± 0.013^{c}	0.050 ± 0.009^{b}	0.015 ± 0.005^{a}	0.107 ± 0.013^{c}	0.472 ± 0.059^{a}	1.030 ± 0.189^{a}	3.536 ± 1.158^{b}	0.471 ± 0.056^{a}
	HC-S	0.026 ± 0.002^{a}	0.058 ± 0.013^{b}	0.030 ± 0.006^{a}	0.071 ± 0.001^{b}	1.906 ± 0.179^{b}	0.893 ± 0.207^{a}	1.712 ± 0.344^{b}	0.705 ± 0.014^{a}
	HC-W	0.159 ± 0.001^{c}	0.118 ± 0.002^{b}	0.049 ± 0.002^{a}	0.197 ± 0.002^{d}	0.314 ± 0.003^{b}	0.425 ± 0.008^{c}	1.017 ± 0.046^{d}	0.254 ± 0.002^{a}
Root	LC-S	0.247 ± 0.034^{b}	0.236 ± 0.011^{b}	0.098 ± 0.015^{a}	0.345 ± 0.015^{c}	0.208 ± 0.029^{a}	0.212 ± 0.009^{a}	0.518 ± 0.083^{b}	0.145 ± 0.060^{a}
	LC-W	0.416 ± 0.007^{b}	0.398 ± 0.007^{b}	0.233 ± 0.020^{a}	0.595 ± 0.003^{c}	0.120 ± 0.002^{b}	0.126 ± 0.003^{b}	0.215 ± 0.018^{c}	0.084 ± 0.001^{a}
	HC-S	0.080 ± 0.019^{a}	0.322 ± 0.023^{c}	0.159 ± 0.005^{b}	0.466 ± 0.048^{d}	0.650 ± 0.159^{c}	0.156 ± 0.011^{a}	0.314 ± 0.009^{b}	0.108 ± 0.011^{a}
	HC-W	0.535 ± 0.005^{c}	0.421 ± 0.006^{b}	0.405 ± 0.001^{a}	0.662 ± 0.001^{d}	0.093 ± 0.001^{b}	0.119 ± 0.002^{c}	0.123 ± 0.001^{d}	0.076 ± 0.001^{a}

LC = low concentration treatment (2 mg/kg soil or mg/L water); HC = high concentration treatment (10 mg/kg soil or mg/L water).
S = Contaminated soil treatment; W = Contaminated water treatment.
CPM = cypermethrin; FVL = fenvalerate; PMT = permethrin; DMT = deltamethrin.
* BCF_t = ratio of pesticide level in plant parts at harvest date to the pesticide level in growing mediums at the time of planting.
** C_s = ratio of maximum pesticide residue concentration limits (MRL) of each pesticide (0.05 mg/kg) to the calculated bioconcentration factor.
[a,b,c,d] Different lower case letters in a row indicate significant differences between mean values evaluated by Duncan's multiple range test ($P < 0.05$).

monitoring pyrethroid concentrations in farmland soils (ND–1.2 mg/kg soil) and water (ND–13.00 mg/L water) worldwide (Tang et al., 2018), the LC-S and HC-W treatments may be better used to study the uptake trend of pyrethroids in other vegetables. To confirm and verify the results from the current study, further experiments should be conducted by growing other types of vegetables or crops.

4. Conclusion

The present study provided a novel prediction method to evaluate the migration of four pyrethroids from the growth media to the vegetable. A double-exponential decline model is recommended as suitable to describe the pyrethroids reductions in growth media, especially the water medium. In terms of plant accumulation, the vegetable could uptake a larger quantity of pyrethroids from the water medium than the soil medium because of the various strength interactions between soil and theses hydrophobic pesticides (Fig. 1). Therefore, using water contaminate with chemical hazards should be taken into account for agricultural production in both global and household scales. Moreover, based on the bioconcentration factors (BCFs), the vegetable could deficiently uptake PMT from the growth media compared to CPM, DMT, and FVL, and its root part demonstrated the superior ability to accumulate pyrethroids in comparison with the sprouting part. The migration of four pyrethroids from the environmental media to the vegetable could be fully studied by the proposed detection method using polystyrene-coated magnetic nanoparticles coupled with HPLC-PDA, even trace amounts of pyrethroids in soil, water, and vegetable matrices were accurately quantified with recoveries of 82.9–112.1%.

CRediT authorship contribution statement

Wanwisa Wongmaneepratip: Conceptualization, Investigation, Methodology, Validation, Formal analysis, Data curation, Writing - original draft. **Hongshun Yang:** Resources, Writing - review & editing, Supervision, Project administration, Funding acquisition.

Declaration of Competing Interest

The authors declare that they have no known competing financial interests or personal relationships that could have appeared to influence the work reported in this paper.

Acknowledgements

This study was funded by the Singapore Ministry of Education Academic Research Fund Tier 1 (R-160-000-A40-114), Natural Science Foundation of Jiangsu Province (BK20181184), and an industry project from Shanghai ProfLeader Biotech Co., Ltd (R-160-000-A21-597).

Appendix A. Supplementary data

Supplementary data to this article can be found online at https://doi.org/10.1016/j.foodchem.2020.128480.

References

Adelsbach, T. L., & Tjeerdema, R. S. (2003). Chemistry and fate of fenvalerate and esfenvalerate. *Reviews of Environmental Contamination and Toxicology, 176*, 137–154.
Ahmed, A. A., Kühn, O., Aziz, S. G., Hilal, R. H., & Leinweber, P. (2014). How soil organic matter composition controls hexachlorobenzene–soil-interactions: Adsorption isotherms and quantum chemical modeling. *Science of The Total Environment, 476-477*, 98–106.
Alsammarraie, F. K., Wang, W., Zhou, P., Mustapha, A., & Lin, M. (2018). Green synthesis of silver nanoparticles using turmeric extracts and investigation of their antibacterial activities. *Colloids and Surfaces B: Biointerfaces, 171*, 398–405.
Bai, W., Zhu, C., Liu, J., Yan, M., Yang, S., & Chen, A. (2015). Gold nanoparticle-based colorimetric aptasensor for rapid detection of six organophosphorus pesticides. *Environmental Toxicology and Chemistry, 34*, 2244–2249.
Bayen, S., Zhang, H., Desai, M. M., Ooi, S. K., & Kelly, B. C. (2013). Occurrence and distribution of pharmaceutically active and endocrine disrupting compounds in Singapore's marine environment: Influence of hydrodynamics and physical–chemical properties. *Environmental Pollution, 182*, 1–8.
Bollag, J.-M., Myers, C. J., & Minard, R. D. (1992). Biological and chemical interactions of pesticides with soil organic matter. *Science of The Total Environment, 123*, 205–217.
Chen, L., Tan, J. T. G., Zhao, X., Yang, D., & Yang, H. (2019). Energy regulated enzyme and non-enzyme-based antioxidant properties of harvested organic mung bean sprouts *(Vigna radiata)*. *LWT, 107*, 228–235.
Eggen, T., Heimstad, E. S., Stuanes, A. O., & Norli, H. R. (2013). Uptake and translocation of organophosphates and other emerging contaminants in food and forage crops. *Environ Sci Pollut Res, 20*(7), 4520–4531.
Fantke, P., Wieland, P., Wannaz, C., Friedrich, R., & Jolliet, O. (2013). Dynamics of pesticide uptake into plants: From system functioning to parsimonious modeling. *Environmental Modelling & Software, 40*, 316–324.
Han, J., Zhou, L., Luo, M., Liang, Y., Zhao, W., Wang, P., Zhou, Z., & Liu, D. (2017). Nonoccupational exposure to pyrethroids and risk of coronary heart disease in the Chinese population. *Environmental Science & Technology, 51*(1), 664–670.
Hanson, B., Hallman, A., Bond, C., & Jenkins, J. (2017). Pesticide binding affinity fact sheet. National Pesticide Information Center, Oregon State University Extension Services. npic.orst.edu/factsheets/bindingaffinity.html. Accessed on 16 May 2019.
Hwang, J. I., Lee, S. E., & Kim, J. E. (2015). Plant uptake and distribution of endosulfan and its sulfate metabolite persisted in soil. *PLoS One, 10*(11), 1–9.
Hwang, J. I., Lee, S. E., & Kim, J. E. (2017). Comparison of theoretical and experimental values for plant uptake of pesticide from soil. *PLoS One, 12*(2), 1–12.
Hwang, J.-I., Zimmerman, A. R., & Kim, J.-E. (2018). Bioconcentration factor-based management of soil pesticide residues: Endosulfan uptake by carrot and potato plants. *Science of The Total Environment, 627*, 514–522.
Juraske, R., Castells, F., Vijay, A., Muñoz, P., & Antón, A. (2009). Uptake and persistence of pesticides in plants: Measurements and model estimates for imidacloprid after foliar and soil application. *Journal of Hazardous Materials, 165*(1-3), 683–689.
Juraske, R., Mosquera Vivas, C. S., Erazo Velásquez, A., García Santos, G., Berdugo Moreno, M. B., Diaz Gomez, J., Binder, C. R., Hellweg, S., & Guerrero Dallos, J. A. (2011). Pesticide uptake in potatoes: Model and field experiments. *Environmental Science & Technology, 45*(2), 651–657.

Koureas, M., Tsakalof, A., Tsatsakis, A., & Hadjichristodoulou, C. (2012). Systematic review of biomonitoring studies to determine the association between exposure to organophosphorus and pyrethroid insecticides and human health outcomes. *Toxicology Letters, 210*(2), 155–168.

Kvesitadze, G., Khatisashvili, G., Sadunishvili, T., & Kvesitadze, E. (2015). In *Plants, pollutants and remediation* (pp. 241–305). Dordrecht: Springer Netherlands.

Laskowski, D. A. (2002). Physical and chemical properties of pyrethroids. *Reviews of Environmental Contamination and Toxicology, 174*, 49–170.

Liu, Y., Li, S., Ni, Z., Qu, M., Zhong, D., Ye, C., & Tang, F. (2016). Pesticides in persimmons, jujubes and soil from China: Residue levels, risk assessment and relationship between fruits and soils. *Science of The Total Environment, 542*, 620–628.

Liu, J., & Schnoor, J. L. (2008). Uptake and translocation of lesser-chlorinated polychlorinated biphenyls (PCBs) in whole hybrid poplar plants after hydroponic exposure. *Chemosphere, 73*(10), 1608–1616.

Mimbs, W. H., IV, Cusaac, J. P. W., Smith, L. M., McMurry, S. T., & Belden, J. B. (2016). Occurrence of current-use fungicides and bifenthrin in Rainwater Basin wetlands. *Chemosphere, 159*, 275–281.

Mishra, T., & Pandey, V. C. (2019). Chapter 16-Phytoremediation of red mud deposit through natural succession. In V. C. Pandey, & K. Bauddh (Eds.), *Phytomanagement of polluted sites* (pp. 409–424). Elsevier Inc.

Nesser, G. A., Abdelbagi, A. O., Hammad, A. M., Tagelseed, M., & Laing, M. D. (2016). Levels of pesticides residues in the White Nile water in the Sudan. *Environmental Monitoring and Assessment, 188*(6), 1–12.

Newcomb, C. J., Qafoku, N. P., Grate, J. W., Bailey, V. L., & De Yoreo, J. J. (2017). Developing a molecular picture of soil organic matter-mineral interactions by quantifying organo-mineral binding. *Nature Communicatons, 8*(1), 396.

Paustenbach, D. J., & Madl, A. K. (2008). The practice of exposure assessment. In A. W. Hayes (Ed.), *Principles and Methods of Toxicology* (Fifth Edition, pp. 475–547). New York: Informa Healthcare USA Inc.

Pereira, V. J., Rodrigues da Cunha, J. P. A., Morais, T. P. D., Oliveira, J. P. R. D., & Morais, J. B. D. (2016). Physical-chemical properties of pesticides: Concepts, applications, and interactions with the environment. *Bioscience Journal, 32*(3), 627–641.

Senesi, N., & Loffredo, E. (2008). The fate of anthropogenic organic pollutants in soil: Adsorption/ desorption of pesticides possessing endocrine disruptor activity by natural organic matter (humic substances). *Journal of Soil Science and Plant Nutrition, 8*, 92–94.

Singapore Food Agency (SFA). (2020). https://www.sfa.gov.sg/newsroom/circulars/maximum-residue-limits-established-for-pesticides-and-veterinary-drugs-previously-not-allowed-in-food. Accessed on 16 May 2020.

Tang, W., Wang, D.i., Wang, J., Wu, Z., Li, L., Huang, M., Xu, S., & Yan, D. (2018). Pyrethroid pesticide residues in the global environment: An overview. *Chemosphere, 191*, 990–1007.

Trapp, S., Cammarano, A., Capri, E., Reichenberg, F., & Mayer, P. (2007). Diffusion of PAH in potato and carrot slices and application for a potato model. *Environmental Science & Technology, 41*(9), 3103–3108.

Wang, Y., Sun, Y., Gao, Y., Xu, B.o., Wu, Q., Zhang, H., & Song, D. (2014). Determination of five pyrethroids in tea drinks by dispersive solid phase extraction with polyaniline-coated magnetic particles. *Talanta, 119*, 268–275.

Xian, Y., Wu, Y., Dong, H., Chen, L., Zhang, C., Hou, X., Zeng, X., Bai, W., & Guo, X. (2019). Modified QuEChERS purification and Fe_3O_4 nanoparticle decoloration for robust analysis of 14 heterocyclic aromatic amines and acrylamide in coffee products using UHPLC-MS/MS. *Food Chemistry, 285*, 77–85.

Yang, T., Doherty, J., Guo, H., Zhao, B., Clark, J. M., Xing, B., Hou, R., & He, L. (2019). Real-time monitoring of pesticide translocation in tomato plants by surface-enhanced Raman spectroscopy. *Analytical Chemistry, 91*(3), 2093–2099.

Yang, T., Zhao, B., Hou, R., Zhang, Z., Kinchla, A. J., Clark, J. M., & He, L. (2016). Evaluation of the penetration of multiple classes of pesticides in fresh produce using surface-enhanced Raman scattering mapping. *Journal of Food Science, 81*(11), T2891–T2901.

Yoo, M., Lim, Y. H., Kim, T., Lee, D., & Hong, Y. C. (2016). Association between urinary 3-phenoxybenzoic acid and body mass index in Korean adults: 1(st) Korean National Environmental Health Survey. *Annals of Occupational and Environmental Medicine, 28*(2), 1–8.

Yu, X., Li, Y., Ng, M., Yang, H., & Wang, S. (2018). Comparative study of pyrethroids residue in fruit peels and fleshes using polystyrene-coated magnetic nanoparticles based clean-up techniques. *Food Control, 85*, 300–307.

Yu, X., & Yang, H. (2017). Pyrethroid residue determination in organic and conventional vegetables using liquid-solid extraction coupled with magnetic solid phase extraction based on polystyrene-coated magnetic nanoparticles. *Food Chemistry, 217*, 303–310.

Zhang, C., Feng, Y., Liu, Y., Chang, H., Li, Z., & Xue, J. (2017). Uptake and translocation of organic pollutants in plants: A review. *Journal of Integrative Agriculture, 16*(8), 1659–1668.

Zimmerman, A. R., Gao, B., & Ahn, M.-Y. (2011). Positive and negative carbon mineralization priming effects among a variety of biochar-amended soils. *Soil Biology and Biochemistry, 43*(6), 1169–1179.